Physica Scripta. Vol. 69, 297–302, 2004

X-ray Reflectivity of Curved Alpha-Quartz Crystals

M. Sánchez del Río[1,*], L. Alianelli[2,3], A. Ya. Faenov[4] and T. Pikuz[4]

[1] European Synchrotron Radiation Facility, BP 220, 38043 Grenoble Cedex, France
[2] INFM-OGG c/o ESRF, BP 56, 38043 Grenoble Cedex, France
[3] Institut Laue Langevin, BP 156, 38042 Grenoble Cedex 9, France
[4] Multicharged Ions Spectra Data Center of VNIIFTRI, Mendeleevo, Moscow region, 141570, Russia

Received June 13, 2003; accepted in revised form December 4, 2003

PACS ref: 41.50.+h

Abstract

X-ray reflectivity curves at 20 keV photon energy of alpha-quartz spherically curved crystals have been measured using a micrometric synchrotron beam at the ESRF BM5. Six thin quartz crystals samples with curvature radii of 150 and 250 mm have been studied. Experimental results are compared with diffraction profile calculations using a lamellar model and a good agreement is found.

1. Introduction

Alpha-quartz is a natural or synthetic hexagonal crystal. Its point group is 32 and its space group is P3221. It is stable below 574.3°C [1]. Above this temperature it changes to beta-quartz. At 867°C it becomes HP-tridymite and finally at 1470°C it changes to beta-cristobalite. It melts at 1727°C. Alpha-quartz monocrystals of quite good quality are not very difficult to find in natural state, and they are widely used for X-ray optics (X-ray monochromators and spectrometers). Different cuts and harmonic orders allow to diffract X-rays in a very wide spectral range [2] from $\lambda = 0.142$ Å ($E \sim 87$ keV), using quartz (502) to 8.12 Å (~ 1.5 keV) using (100).

For X-ray spectrometers and X-ray imaging applications, it is interesting to curve the crystal surface to a spherical, cylindrical or toroidal shape, in order to focus monochromatic radiation into a focal line or point. These spectrometers require a high crystal perfection and a very good optical accuracy of the crystal surface. A method to obtain such a crystal is to cut a plane thin (50–100 μm) layer of quartz along a particular crystallographic direction and bond it to a polished glass substrate [3]. These crystals are widely used for applications in association with plasma X-ray sources: plasma analysers [4], backlighting schemes [5–7], etc. They can also be used to exploit the plasma sources as X-ray sources for different applications, e.g., quartz curved crystals can be used to produce quasi-parallel (with divergence up to 1 mrad) beams by using a plasma source [8], and for microscopy applications [9–11]. Many commercial spectrometers working with conventional X-ray tube generators are equipped with quartz crystals.

In this work we present X-ray reflection profiles for different quartz crystals of thickness about 60 μm curved to spherical shape with curvature radii of 150 and 250 mm. These crystals have been used in plasma applications. The objective of this study is to record experimental information that could help in assessing the usability of these crystals for a given application. In addition, we wanted to study if the crystal quality is good enough that the experimental reflectivity could be accurately predicted using theoretical models.

From the experimental point of view, the diffraction profile should be measured by rocking the crystal using a monochromatic pencil (collimated and with infinitesimal cross section) X-ray beam. These conditions are very difficult to match using conventional X-ray sources, therefore, it is difficult to find experimental results in literature. When using curved crystals with rather high curvatures ($R \sim 10$ mm), the incident beam cross section in the diffraction plane is particularly critical, because it produces an angular spread when projected onto the crystal surface, and this spread must be kept smaller than the width of the diffraction profile. The extraordinary characteristics of monochromacity and collimation of the synchrotron beam make it appropriate for this type of measurements. Moreover, the beam cross section can be reduced to a micrometric size using a guard slit, keeping a beam intensity high enough to perform rocking curve measurements. Additionally, X-rays can be tuned to the desired wavelength. The measurements results will be compared with the lamellar theory, which consist in assuming a bent crystal made from thin layers of perfect crystal (where dynamical theory applies) and then the effect of the curvature in the reflectivity is seen by (incoherently) adding the contribution of the lamellae.

2. Experimental

The experiments were performed at the ESRF beamline BM5. The source was a bending magnet with critical energy of 19 keV. The beamline is equipped with a double plane crystal Si (111) monochromator delivering a monochromatic beam (20 keV) with an energy resolving power $E/\Delta E$ of about 10^4. An entrance slit upstream from the sample defined a beam cross section of 8 μm (horizontal) and about 1 mm (vertical).

The quartz samples were mounted in a diffractometer. The diffraction plane was horizontal. The rocking curves were measured by performing a θ-2θ scan. A silicon diode detector was used to record the diffracted intensity. The rocking curves were normalized using the direct beam intensity counting, thus obtaining values of absolute reflectivity. Four quartz samples with curvature radius of $R = 150$ mm cut along the Bragg planes with Miller indices

* e-mail: srio@esrf.fr

of (100), (110), (203) and (011) and two more samples with $R = 250$ mm with (100) and (011) were studied. Note that our notation (hkl) is equivalent to the often used notation ($hkil$) where $i = -(h + k)$. The crystal wafers had a thickness of approximately 60 μm and an optical surface of about $1 \times 1\,\text{cm}^2$. They were prepared by gluing the wafers to an optically polished glass substrate. The selected quartz crystals have passed optical tests before being processed. They correspond to Grade 1 quality. The bending process does not alter the quality of the crystals, as it was shown in [12] for the case of mica crystals.

The main parameters of the experimental results (peak reflectivity, full-width at half-maximum (FWHM) and integrated intensity) are summarized in Table I. The experimental rocking curves have a typical triangular or trapezoidal shape (see Fig. 1). In both cases, the atomic layers placed closer to the crystal surface reflect stronger. They are responsible for the peak reflectivity values. The atomic layers that are found deeper in the crystal bulk are slightly disoriented (non-parallel) with respect to those close to the surface, due to the curvature. Therefore, the beam arrives onto them with a slightly different incident angle. In addition, the attenuation is more important for deeper layers, thus giving lower reflectivity. This explains the triangular profile. In the particular case that the crystal is thinner than the distance that the beam would penetrate into the crystal, a part of the "triangle" is missing, and the profile shows a trapezoidal shape.

The experimental rocking curve is a convolution of the diffraction profile with the beam divergence. With an ideal pencil beam (no divergence, zero cross section, and infinite resolving power), both the rocking curve and the diffraction profile match perfectly. The width of the diffraction profile for a bent crystal is several times the Darwin width. In our case, it is of the order of a mrad, depending on the curvature, thickness, and Miller indices (or Bragg angle). It is then crucial to reduce the overall beam divergence to quantities of this order or smaller. The effective beam divergence comes from two factors: (*i*) the divergence of the photon beam Δ_1, which is negligible in our case ($\Delta_1 =$ (slit size)/(source distance) $= 8 \cdot 10^{-6}/40$), and, (*ii*) the angular spread produced by the projection of the beam cross

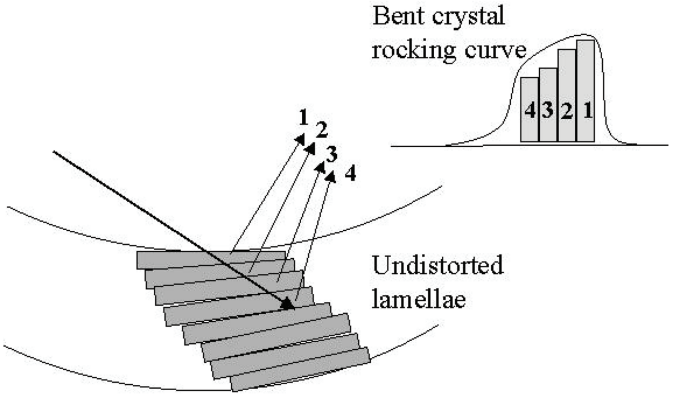

Fig. 1. Schematic representation of the lamellar model. The bent crystal is divided into many undistorted layers whose orientations follow the curvature of the Bragg planes. The diffraction profile is wider than the perfect crystal one, because different orientations of the incident beam can satisfy the Bragg's law at different depths.

section onto the curved crystal surface. The latter produces a dispersion of the Bragg angle with a value of $\Delta_2 = (s/\sin\theta_B)/R$, s being the size of the entrance slit in the direction of the diffracting planes, θ_B the Bragg angle and R the bending radius. In our case, $s = 8\,\mu\text{m}$, $\theta_B > 4$ deg, $R \geq 150$ mm, thus the added divergence is, in the worst case, about $8 \cdot 10^{-4}$, i.e., 45 mdeg.

Our samples show a very uniform curvature, demonstrated by their performances in other applications. We have tested the crystal curvature by comparing two diffraction profiles: (*i*) one recorded in the usual θ-2θ scan, and (*ii*) keeping fixed the incident beam and moving the crystal along a direction perpendicular to the crystal surface, and which lies in the diffraction plane. Therefore, the grazing angle changes continuously due to crystal curvature. Both profiles appear to have identical shapes.

3. Calculation of diffraction profiles

Diffraction of X-rays by flat undistorted crystals is well understood in terms of the dynamical theory of diffraction [13–16]. The extension of the dynamical theory to treat deformed crystals has been formulated and treated by many authors. See [17] for a recent and complete review.

Table I. *Peak reflectivity, rocking curve FWHM integrated intensity [deg] from experimental rocking curves. The Bragg angle is also indicated.*

R [m]	Reflection	Peak	FWHM [deg]	Integrated Intensity	θ_B [deg]	Sample number
150	011	0.123	0.162	$20.5\ 10^{-3}$	5.32	5
	022	0.016	0.129	$1.85\ 10^{-3}$	10.69	
	203	0.033	0.077	$2.5\ 10^{-3}$	13.03	4
	110	0.022	0.189	$3.55\ 10^{-3}$	7.25	
	220	0.0114	0.104	$1.13\ 10^{-3}$	14.62	3
	330	0.0021	0.066	$0.13\ 10^{-3}$	22.20	
	200	0.0185	0.150	$2.49\ 10^{-3}$	8.57	
	300	0.0026	0.100	$0.24\ 10^{-3}$	12.79	1
	400	0.0037	0.072	$0.25\ 10^{-3}$	16.00	
250	011	0.191	0.136	$23.5\ 10^{-3}$	5.32	6
	022	0.027	0.073	$1.88\ 10^{-3}$	10.69	
	100	0.048	0.152	$7.46\ 10^{-3}$	4.18	
	200	0.032	0.108	$2.96\ 10^{-3}$	8.38	2
	300	0.051	0.071	$0.32\ 10^{-3}$	12.62	
	400	0.0074	0.052	$0.35\ 10^{-3}$	16.94	

Most methods start from Takagi's [18] differential equations, which include a term to deal with deformations. These equations have (complicated) analytical solutions in only few cases, and are usually treated by numerical integration. Curved crystals can in most cases be treated as a particular slight depth-dependent-only deformation, which allows to write the Takagi equations as a second degree ordinary differential equation [19] that can be numerically integrated. Some computer programs use this method [20]. However, a very simple computational model (hereafter called the *lamellar* model) was used to compute curved crystal neutron diffraction profiles [21–23]. The lamellar method was also applied to X-ray diffraction and its results checked against the original results of Taupin [24]. The model was successfully used for X-ray applications [25–27]. A computer program using this and other methods for curved crystals [28] was developed and is freely available [29]. We have used this code for the analysis presented here.

The main idea of this method is to decompose the crystal (in the direction of beam penetration) into several layers of a suitable thickness. Each layer behaves as a perfect crystal thus the diffracted and transmitted beams are calculated using the dynamical theory for plane crystals. The different layers are misaligned one with respect to the others in order to follow the curved surface of the crystal plate.

An angular parameter y (related to the deviation of the incident angle from the Bragg angle) is assumed to be a function of the depth from the crystal entrance surface for a fixed direction of the incident beam. At the entrance surface the y value is called y_0 and is identical to the "y" variable of Zachariasen [14]. The Darwin perfect crystal profile, in Bragg geometry, without absorption, has an angular width of $2y_0$. A given angular difference τ from the Bragg angle will have an y_0 value of:

$$y_0 = \frac{\frac{1-b}{2}\Psi_0 + \frac{b}{2}\tau}{\sqrt{|b|}P|\Psi_H|} \tag{1}$$

where b is the asymmetry factor, Ψ_H is the Fourier component of the electrical susceptibility Ψ_0, and P is the polarization factor. For a crystal with cylindrical curvature in the diffraction plane (this includes the spherical case) of radius R, and a thickness t it holds $y = y_0 + cA$, where A is the reduced thickness defined as:

$$A = \frac{\pi P|\Psi_H|}{\lambda\sqrt{|\sin(\theta_B - \alpha) + \sin(\theta_B + \alpha)|}}t \tag{2}$$

where α is the asymmetric angle. The parameter c is a dimensionless quantity related to R through:

$$c = \frac{\sin(\theta_B - \alpha)(b-1)}{\pi|\Psi_H|^2 bR}[1 + b(1+\nu)\sin^2(\theta_B + \alpha)] \tag{3}$$

where ν is the Poisson ratio of the used material. Each perfect slab has a reduced thickness $\Delta A = 2/c$ and a misorientation $\Delta y = 2$ relative to the adjacent ones. In other words, the reflecting profiles of the individual layers will pile one close to another under the hypothesis that their width is $2y_0$. This is a reasonable condition only in the case of thick crystal approximation for the individual layer. If the layer is thinner than a given quantity (extinction depth) the width of the perfect crystal diffraction profile becomes broader. The total reflectivity of the given set of layers can be computed by writing the energy balance for the different layers, which leads, in the case of n layers to:

$$\frac{I}{I_0} = \sum_{j=1}^{n} r_j \left(\prod_{k=0}^{j-1} t_k \exp(-\mu S_k) \right) \tag{4}$$

where S_k is the X-ray path inside the kth layer, μ is the absorption coefficient of the crystal material, r_i and t_i are the (power) reflectivity and transmission ratio for the ith layer, respectively. Validity and limitations of this model have been analysed in literature [25,27,30]. We can summarise them as:

1. The crystal deformation (radius of curvature) is small (large) enough to assume that the individual layers are perfect crystals.
2. The crystal must be "thick" enough to guarantee that a "sufficient" number of layers contribute to the total reflectivity.
3. The incident beam path inside the crystal is a straight line (not always true, see [31]).
4. The model supposes that the width of the individual layer profile is $2y_0$, thus "thick" crystal approximation applies. This is a good approximation for small values of c (proportional to $1/R$), typically 10 to 100. If c becomes large, it implies that each layer for $\Delta y_0 = 2$ will be very thin. A very large number of layers will be needed, each layer contributing to a small amount of final intensity. Large values of c typically occur for high curvatures or high reflection orders. Although this is an important limitation of the model, as pointed out by [30], we obtained good agreement with experiment also in these cases.

From the practical point of view, we shall consider now how the simulation parameters affect the resulting diffraction profile. The width of the profile depends on the crystal curvature and thickness. The thickness may have a "cutting" effect in the left edge of the profile, resulting from the fact that crystal material that would diffract in the thick case is missing. The slope of the profile's "ceiling" depends on the absorption coefficient. A more pronounced slope means more absorption. Zero absorption would give horizontal curves.

A very important factor to consider is the temperature factor, $DW = \exp(-M)$, which multiplies the structure factor, the main ingredient of Ψ_H. Computation of accurate values of the temperature factor is cumbersome, and a "simple" Debye–Waller term is usually applied (even in the case that this is only valid for cubic lattices):

$$\begin{aligned} DW = \exp(-M) &= \exp(-(B_0 + B_T)(\sin\theta_B/\lambda)^2) \\ &= \exp(-B/(2d)^2) \end{aligned} \tag{5}$$

where $B_0 = 3h^2/2k_B T_D A$, with h denoting Planck's constant, k_B the Boltzmann constant, T_D the Debye temperature and A the average atomic mass number. The B_T term is temperature-dependent: $B_T = 4B_0\phi(x)/x$ where

x is the ratio temperature over the Debye temperature ($x = T/T_D$) and $\phi(x) = x^{-1}\int_0^x \xi\, d\xi/(e^{+\xi} - 1)$. Clearly, high harmonic reflections (smaller d-spacing) will reduce the DW factor significantly. This has a dramatic effect on the peak intensity of the calculations. As a matter of fact, DW can be used as an "adjustable" parameter in the simulations. This is also justified because there is no agreement on the values of the Debye temperature in literature. In our case, we found that the value of DW used to agree with experimental results is about 5–10% smaller than the one calculated using numerical values for quartz listed in [32].

Figure 2 shows the parametric dependence of the calculated diffraction profile. We show that the temperature factor contributes to the diffraction profile in a vertical scaling. A change in curvature radius will affect both the peak value and the width of the curve. The crystal thickness only affects the width (for thick crystals, where the shape of the profile is trapezoidal), and the absorption coefficient affects the slope. Regarding the absorption coefficient, we see a small effect in the profile slope for variations of ±20% of the nominal value. The effect of the absorption coefficient is therefore less important as compared with the other parameters. In our simulation, we have calculated it starting from the photoelectric cross section, meaning that absorption and scattering due to inelastic processes (basically Compton) are neglected. The inelastic cross section for quartz at 20 keV amounts to less than 6% of the total cross section, so the fact of neglecting inelastic processes is well justified.

4. Comparison experiment-theory

The experimental rocking curves have been compared with calculated diffraction profiles. See Fig. 3 and Table II. The procedure was to compute the diffraction profile for the given reflection using a thickness of 60 μm and a DW as calculated using formula (5) with a mean atomic mass of $A = 20.03$ and Debye temperature of $T_D = 500$ K [32]. Then, the calculated profile was convoluted with a Gaussian of FWHM equal to $\Delta_2 = (s/\sin\theta_B)/R$ in order to take into account the angular spread of the beam onto the crystal due to curvature. In most cases, two parameters were manually refined (not fitted) to arrive at a better agreement. These parameters were DW and crystal thickness. DW controls the peak value and usually the adjusted values were about 5–10% smaller than the first predictions. The crystal thickness was changed to improve the agreement in width. Although the nominal thickness of the samples is 60 μm, no precise measurements on this value (nor on the curvature radius)

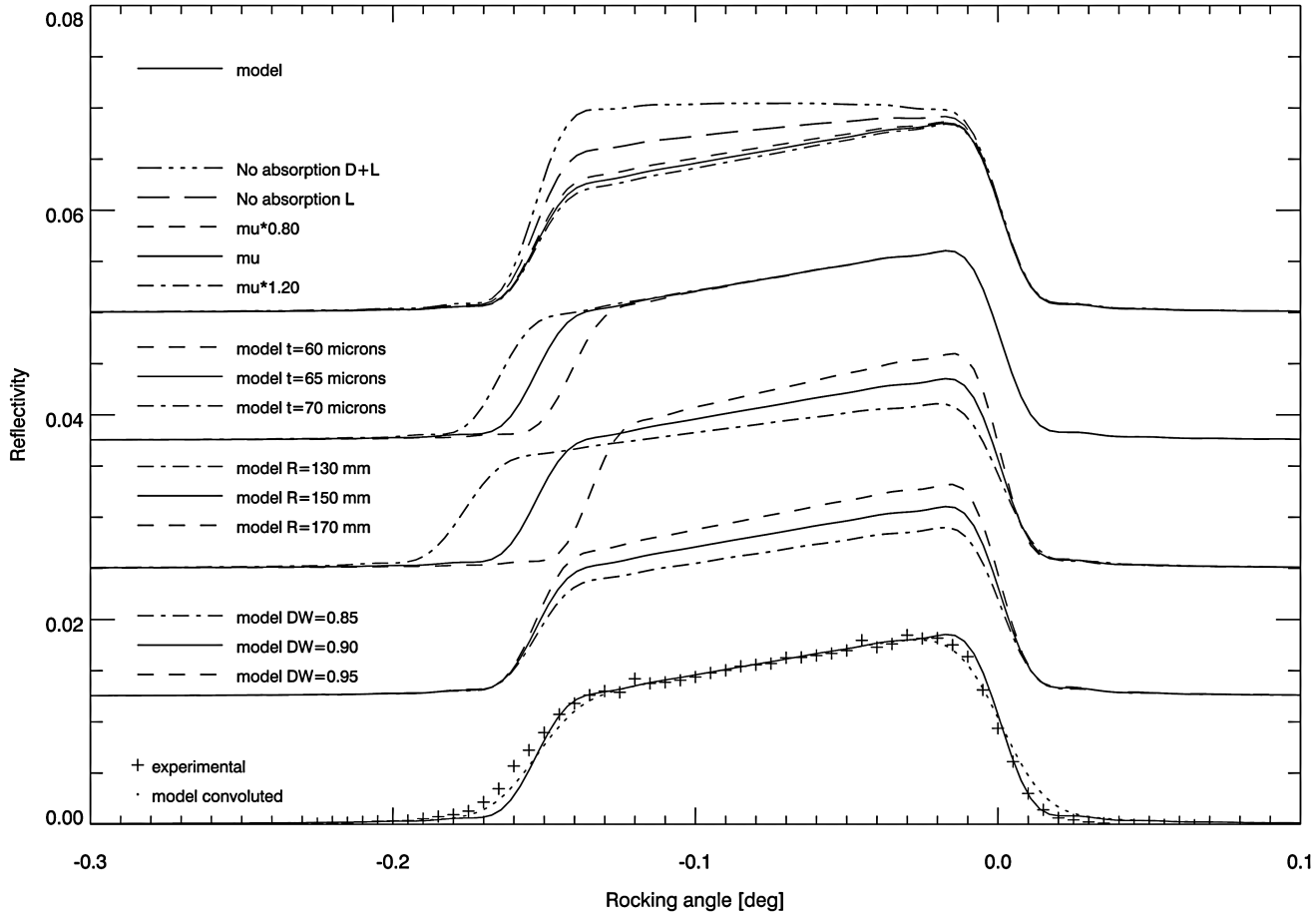

Fig. 2. This figure shows the calculation parameters (temperature factor DW, radius of curvature R, crystal thickness t and absorption coefficient μ) influence on the diffraction profiles. The solid line is the reference model calculation (using $DW = 0.90$, $t = 65$ μm, and $\mu = 5.78\,\text{cm}^{-1}$) for bent quartz with $R = 150$ mm at 20 keV using the (200) reflection. From bottom to top: (1) Experimental points (plus sign), model (solid) and model convoluted with a Gaussian of 0.021 deg FWHM (dotted). (2) Effect of change in DW. (3) Effect of change in curvature radius. (4) Effect of change in crystal thickness. (5) Effect of change in absorption coefficient. Here, "No absorption D + L" means that absorption is neglected in both the dynamical theory calculation of the single lamella profile, and in the lamella model (formula (4)). "No absorption L" means that absorption is considered for the dynamical calculation and neglected in the lamella model. Some curves have been shifted in vertical for clarity.

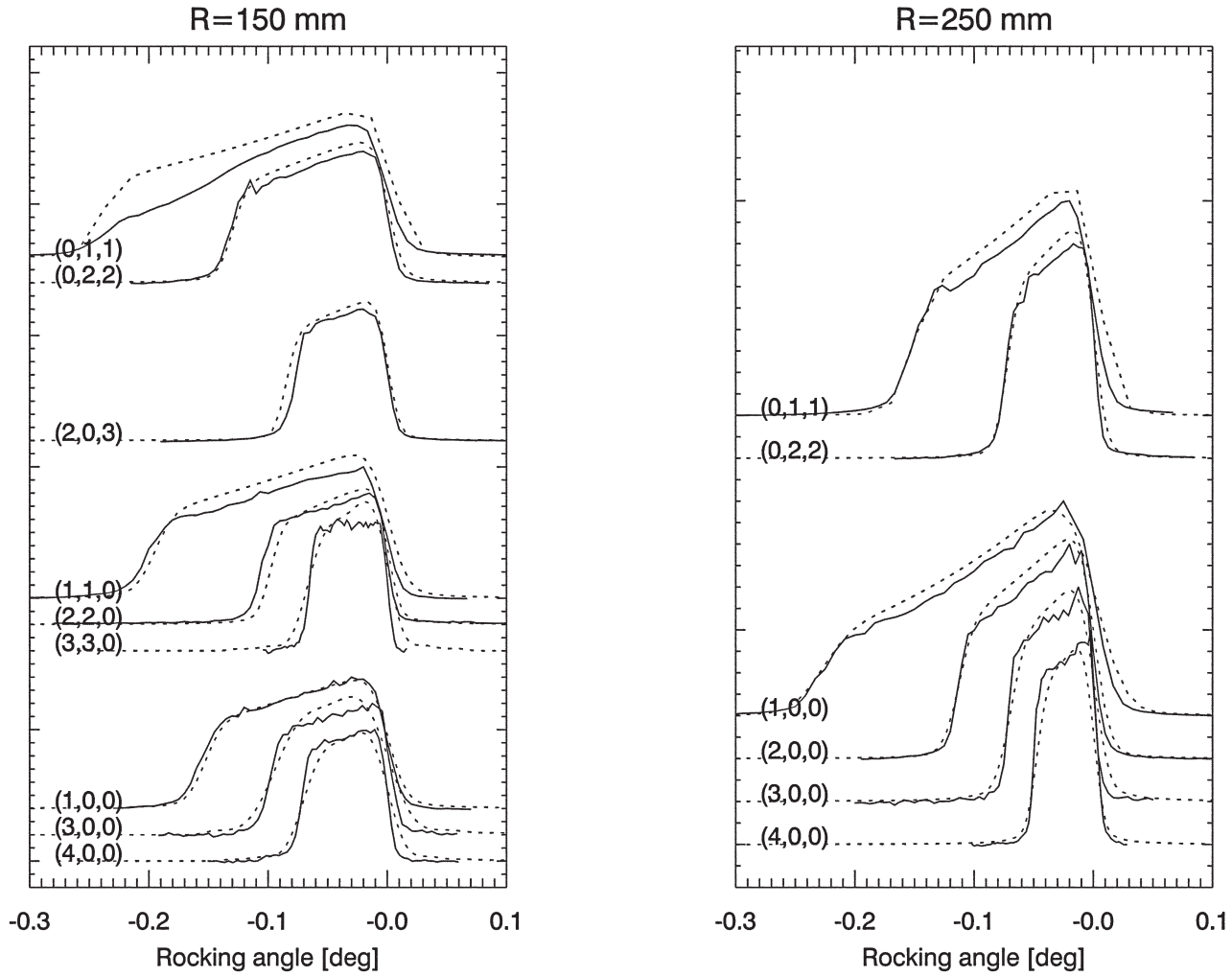

Fig. 3. Experimental (solid line) and simulation (dotted line) results for the six bent quartz samples studied (four bent with a curvature radius $R = 250$ mm and two with $R = 250$ mm), for a number of diffracting planes. Experimental rocking curves are normalized in height (their absolute peak values are given in Table I), and simulations are directly compared. The parameters used in the simulations are listed in Table II. The vertical origins of the curves have been shifted for clarity.

were done, and the values could change from one crystal to another. It is therefore justified to readjust this parameter. For practical purposes, an adjustment of the thickness could also imply a change in R, as the parameters are correlated in

Table II. *Parameters adjusted for the numerical calculation of the diffraction profile in order to agree with experimental profiles. Graphical results are shown in Fig. 3. The Δ_2 value is the FWHM of the Gaussian function used for convolution of the calculated diffraction profile for including angular spread on the crystal surface. The Bragg angle and the* c *parameter (see text) are also included.*

R [m]	Reflection	Thickness [μm]	DW adjusted	DW theory	Δ_2 [deg]	θ_B [deg]	c	Sample number
	011	60	0.95	0.984	0.033	5.32	18	5
	022	75	0.88	0.936	0.016	10.69	160	
	203	65	0.80	0.907	0.014	13.03	78	4
	110	70	0.95	0.970	0.024	7.25	112	
150	220	90	0.82	0.885	0.012	14.62	227	3
	330	150	0.65	0.759	0.008	22.20	1039	
	200	65	0.90	0.960	0.021	8.57	148	
	300	70	0.85	0.912	0.014	12.79	929	1
	400	85	0.75	0.854	0.011	16.00	714	
	011	65	0.95	0.983	0.033	5.32	11	6
	022	70	0.90	0.936	0.016	10.69	92	
	100	75	0.95	0.990	0.042	4.18	51	
	200	80	0.95	0.960	0.021	8.38	79	2
	300	85	0.90	0.912	0.014	12.62	497	
	400	90	0.80	0.849	0.010	16.94	376	

the final calculated profile. The same applies to DW and the absorption coefficient. For most cases the variations in thickness were about 10–20% of the nominal values. It is however remarkable, that in one particular case (reflection (330)) the thickness had to be increased to $t = 150\,\mu m$ in order to adjust the width to the experimental value. We do not have a sensible explanation for that. It could be that the model fails for this reflection ($c \sim 1039$) but in other cases, also with large c ($c \sim 929$ in (300) $R = 150\,mm$) reasonable results are obtained. However, the dispersion of the adjusted thickness values with respect to the nominal one seems to be more accentuated than what we expected for real variations in thickness. Whether this "effective" thickness could take into account other sources of inaccuracies would need further studies. It is interesting to point out that similar problems have been found when applying the lamellar method [15,24] to the study of neutron diffraction profiles for bent germanium crystals [33].

5. Conclusion

This work presented an experimental and numerical study of alpha-quartz rocking curves at 20 keV. The dependence of the diffraction profiles on the curvature radius, crystal thickness, absorption coefficient, temperature factor and other parameters has been studied using a lamellar computer model. Experimental results have been compared with simulations with quite good agreement, although in one case an exaggerated thickness was found. It is remarkable that the model gives good results even for high values of the c parameter, contrary to what was expressed in literature. It was found essential to include good values of the temperature factor in order to get good experimental-theory agreement. It can be concluded that the lamellar model is a robust method to *ab initio* compute diffraction profiles of alpha-quartz bent crystals used in monochromators and spectrometers.

Acknowledgement

We acknowledge the ESRF BM5 staff for their support during the experimental measurements.

References

1. Keen, D. A. and Dove, M. T., J. Phys. Condens. Matter **11**, 9263 (1999).
2. Thompson, A. C. and Vaughan, D. (Lawrence Berkeley National Laboratory, Berkeley, 2001).
3. Boiko, V. A., Vinogradov, A. V., Pikuz, S. A., Skobelev, I. Y. and Faenov, A. Y., Sov. J. Laser Res. **6**, 82 (1985).
4. Skobelev, I. Y. *et al.*, J. Exp. Theor. Phys. **81**, 692 (1995).
5. Pikuz, S. A. *et al.*, SPIE proceedings **2520**, 330 (1995).
6. Sanchez del Rio, M. *et al.*, Physica Scripta **55**, 735 (1997).
7. Aglitskiy, Y. *et al.*, Appl. Opt. **37**, 5253 (1998).
8. Sánchez del Rio, M., Fraenkel, M., Ziegler, A., Faenov, A. Y. and Pikuz, T. A., Rev. Sci. Instrum. **70**, 1614 (1999).
9. Fraenkel, M., Zigler, A., Faenov, A. and Pikuz, T., Physica Scripta **59**, 246 (1999).
10. Sánchez del Rio, M., Alianelli, L., Pikuz, T. A. and Faenov, A. Y., Rev. Sci. Instrum. **72**, 3291 (2001).
11. Pikuz, T. A. *et al.*, Laser Particle Beams **19**, 285 (2001).
12. Hölzer, G. *et al.*, Physica Scripta **57**, 301 (1998).
13. James, R. W., "The optical principles of the diffraction of X-rays." (G Bell & Sons, London, 1950).
14. Zachariasen, W. H., "Theory of X-ray diffraction in crystals." (Dover, New York, 1945).
15. Batterman, B. W. and Cole, H., Rev. Mod. Phys. **36**, 681 (1964).
16. Pinsker, Z. G., "Dynamical scattering of X-rays in crystals." (Springer Verlag, Berlin, 1978).
17. Authier, A., "Dynamical theory of X-ray diffraction." (Oxford University Press, Oxford, 2001).
18. Takagi, S., J. Phys. Soc. Jap. **29**, 1239 (1969).
19. Taupin, D., Bull. Soc. Fr. Minér. Crist. **87**, 469 (1964).
20. Hölzer, G., Wehrhan, O. and Förster, E., Crys. Res. Technol. **33**, 555 (1998).
21. White, J. E., J. Appl. Phys. **21**, 855 (1950).
22. Egert, G. and Dachs, H., J. Appl. Cryst. **3**, 214 (1970).
23. Albertini, G. *et al.*, Acta Cryst. **A 32**, 863 (1976).
24. Boeuf, A. *et al.*, J. Appl. Cryst. **11**, 442 (1978).
25. Caciuffo, R., Melone, S., Rustichelli, F. and Boeuf, A., Phys. Rep. **152**, 1 (1987).
26. Suortti, P., Pattison, P. and Weyrich, W., J. Appl. Cryst. **19**, 336 (1986).
27. Erola, R., Eteläniemi, V. and Suortti, P., J. Appl. Cryst. (1990).
28. Sánchez del Rio, M., Ferrero, C. and Mocella, V., SPIE proceedings **3151**, 312 (1997).
29. Sánchez del Rio, M. and Dejus, R. J., SPIE proceedings **3448**, 230 (1998).
30. Chantler, C. T., J. Appl. Cryst. **25**, 674 (1992).
31. Gronkowski, J. and Malgrange, C., Acta Cryst. **A 40**, 507 (1984).
32. Freund, A. K., Nucl. Instr. and Meth. **213**, 495 (1983).
33. Alianelli, L., Thesis, Université Joseph Fourier, Grenoble, (2002).

